cigre Turkey

TEPES
TURKISH JOURNAL OF ELECTRICAL POWER AND ENERGY SYSTEMS

TEPES, Vol. 2, Issue. 1, 21-30, 2022 DOI: 10.5152/TEPES.2022.21048

RESEARCH ARTICLE

Online Parameter Identification of a Simplified Composite Load Model by Voltage Sag Events

Mehmet Karadeniz[1], **M. Timur Aydemir**[2], **Saffet Ayasun**[3]

[1]Department of Electrical and Electronics Engineering, Kyrgyz-Turkish Manas University, Bishkek, Kyrgyzstan
[2]Department of Electrical and Electronics Engineering, Kadir Has University, İstanbul, Turkey
[3]Department of Electrical and Electronics Engineering, Gazi University, Ankara, Turkey

Cite this article as: M. Karadeniz, M. T. Aydemir & S. Ayasun. Online parameter identification of a simplified composite load model by voltage sag events. *Turk J Electr Power Energy Syst,* 2022; 2(1): 21-30.

ABSTRACT

Monitoring power quality events that occur in a power grid and determining their causes are important in terms of taking preventive actions. Power quality events are generally caused by structural changes in the network. Network loads are also affected by power quality events as a part of the network or they may cause power quality events themselves due to a sudden change in their structure. In this respect, when a power quality event occurs, the estimation of the behavior of the network loads contributes to the determination of the causes of the power quality events. In this study, a new method is developed to identify the parameters of a composite load model to estimate the response of network loads to certain power quality events. The method identifies model parameters using the voltage sag or swell data. By this model, it is possible to estimate the response of the loads and detect whether there is a change in the load. In this way, it becomes easier to understand whether the event is caused by the load or the network, which eventually helps us find the causes of power quality events. Simulation studies show that the load parameters identified by the method using a voltage sag are close to the actual load parameters, and the load behavior estimated by the load model in case of any power quality event is very close to the real load.

Index Terms—Voltage sag/swell, composite load modeling, parameter identification, power quality

I. INTRODUCTION

Power quality issues have been drawing a lot of attention in modern power systems. For customers to sustain quality service, the identification of events that negatively affect power quality is crucial to reduce their adverse effects. Observed power quality events as transients distort waveforms within the network. Voltage dips, transients, peeks, or voltage fluctuation is types of power quality problems. These events reduce the quality of the power supplied to the customers and have negative effects on other components and devices in the network. In order to take the necessary precautions against power quality events, it is vital to determine the types and causes of power quality problems. Power quality is defined as "a set of electrical boundaries that allows an equipment to function in its intended manner without significant loss of performance or life expectancy[1]."

Events affecting the power quality in the network are generally caused by structural changes such as changes in network lines or network loads. In order to find the causes of an event, possible scenarios should be examined and their results should be compared. For that purpose, a load model that can estimate the response of loads to events is contributive to analyzing an event. As a result of an event in the network, when the voltages at certain points of the network go beyond the normal operating range, obtaining a model that can accurately estimate the instantaneous response also has the following important advantages: (1) providing the status and characteristics of network loads and (2) allowing the detection of the changes in the loads in the network, thus making it possible to observe the changes of these loads over time. Having a load model for each load on the grid, it will be easier to determine if there is a change in the grid and at what point the change occurred.

In the literature, there are studies on several load models. Polynomial model or constant impedance (Z), constant current (I), constant power (P) (ZIP) model is one of the first among these load models based on the assumption that a load is composed of constant impedances, constant current, and constant power drawing components [2]. However, it is a static model and does not take

Corresponding author: Saffet Ayasun, saffetayasun@gazi.edu.tr

Received: November 26, 2021
Accepted: February 14, 2022

into account the load dynamics. There are studies in which the ZIP model and induction motor model are used to model dynamics of load, which is called composite load [3-5]. In these models, there are difficulties in parameter identification. To overcome these difficulties, a simplified composite load model is presented which consists of only one impedance and an induction motor [6-9]. The parameters of this model can be obtained using data from a detected power quality event. Another form of a load model is the transfer function-based load model [10]. More recent studies dedicated to Western Electricity Coordinating Council (WECC) [11-13] were encountered to more severe identification problems. However, WECC composite load model has too many parameters, an effort to reduce the number of parameters is needed [14].

Apart from the accurate model selection, method selection is also another consideration. There are several methods used in parameter identification mainly based on statistical and heuristic techniques. In the group of statistical methods, there are weighted least square-based estimation [15], least square-based parameter estimation [16], and maximum likelihood-based estimation [17]. In the group of heuristic methods, there are genetic algorithms [18], neural networks [19], and simulated annealing algorithms [20]. In [21], it was reported that: (1) the maximum likelihood approach was a time-consuming task, and the probability density function of measurements is needed to define the likelihood function, which may be unknown in practice and (2) The gradient-based approach was vulnerable to data pollution. Although the genetic algorithm is a multi-point search algorithm and can be adapted to different problems, it requires too much computation. Artificial neural networks can be trained with measurement data without requiring knowledge of the structure of the load model. However, the convergence rate of this method is quite slow. The simulated annealing method does not require the knowledge of the structure of the load model. However, the repeated annealing process is slow.

Based on the discussion given above, this study aims to obtain the load model as quickly as possible and to examine the causes of the events, and for this reason, the focus is given on the simple composite load model. The simplified composite load model is based on the assumption that a grid load can be modeled with an impedance and an induction motor. According to the study of Savio et al., many induction motors connected to a bus behave like a single induction motor [22]. Accordingly, it is understood that a real load consisting of *N* number of induction motors and *M* number of impedance loads can be modeled with an induction motor and an impedance connected with each other in parallel.

Main Points

- The effect of power quality events on the load model and dynamics.
- A new method to identify composite load parameters using voltage sag or swell data.
- Fast identification of composite load parameters and model with sufficient accuracy.

There are studies on identifying the parameters of the simplified composite load model. In [3] and [23], an online method was proposed based on parameter tuning. In [7], the most important parameters of the composite load were identified with a two-step approach. In these methods, the identification process has calculation loops: amount of impedance and motor parts of the load are obtained after the trial-and-error process. Power quality events occur frequently and it is possible for an event to affect the load and causes permanent changes in the load. In this case, when a power quality event occurs, the load model will need to be determined quickly. Therefore, while these methods mentioned can be used in stability analysis, they may not be fast enough to catch up with power quality events. For this reason, the main purpose of this study is to develop a less sensitive but faster method.

In this study, a method has been developed in which model parameters can be identified with the data of voltage sag or swell that occurred in the network. The model consists of an impedance in which the resistance and inductance are connected in series and an induction motor connected in parallel. This aggregated load model is able to estimate the response of a load to events that occurred, and more generally to estimate the current drawn. An event that occurred in the network causes instantaneous changes in the voltage of the load, and the current drawn by the load can be estimated by the proposed approach. Once the parameters of the model have been identified, the load response to new events can now be estimated, and whether there is a change in the load in each event can be determined with the available measurement data. The parameters of the model are identified by the data of voltage drop events. The model of which parameters are identified by the method can estimate the load response for any event that may occur afterward. With this method, the impedance part of the load and the important parameters that affect the motor dynamics are determined. Compared to the studies in the literature, it is observed that these parameters are obtained with less computational effort in a shorter time. By comparing the estimation results obtained with the response of the actual load, it can be determined whether the load has changed in the following events. Furthermore, by including the load model in the network model, events that may occur in the network can be examined. The most important advantage of the method is that the process of parameter determination provides the result in a short time and with less processing. With this method, load parameters are identified with a certain error rate and the response of the load can be estimated successfully. The amount of error in the determination has little negative effects on estimating the response of the load. Therefore, the results of the method can be used directly in estimating the response of the load or the values identified by this method can provide initial values to other methods.

II. COMPOSITE LOAD MODEL

The simplified composite load model takes impedance and motor loads into account. In Fig. 1, the structure of the composite load recommended by IEEE is presented [25]. Note that the composite load model consists of a static impedance load and an equivalent induction motor part. The equivalent induction motor part of this model has been developed by neglecting the stator transients based on the dynamic model of the induction motor and was generally used in

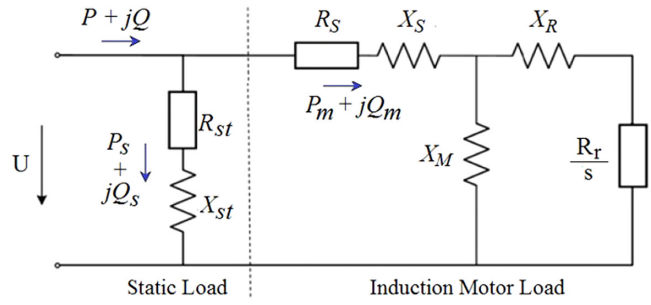

Fig. 1 . Simplified composite load structure and circuit.

system stability studies [24, 25]. The state equations of equivalent induction motor can be written as:

$$\begin{aligned}\frac{dE_d}{dt} &= -\frac{1}{T_0'}\left(\frac{X}{X'}E_d - \frac{X-X'}{X'}U_d\right) + \omega_0 s E_q \\ \frac{dE_q}{dt} &= -\frac{1}{T_0'}\left(\frac{X}{X'}E_q - \frac{X-X'}{X'}U_q\right) - \omega_0 s E_d \\ \frac{ds}{dt} &= -\frac{1}{H}\left(P_{mt} - P_{mt0}\left(A\omega_r^2 + B\omega_r + C\right)\right)\end{aligned} \quad (1)$$

where

$$X' = X_S + X_M // X_R;\ T_0' = \frac{\left(X_M + X_R\right)}{\omega_0 R_r};\ X = X_S + X_M;\ A + B + C = 1 \quad (2)$$

There are many parameters to be determined in this model and it is very difficult to determine all of them. Here, some assumptions can be made to simplify and thus, the reduced number of parameters are to be determined. It is stated in the literature that the effect of the stator resistance R_s, the magnetization impedance X_M, and the mechanical coefficients A, B, and C on the electromechanical dynamic characteristics of the motor is quite low [7]. These parameters, which have little effect on the load, can be excluded from the load model, and this simplifies parameter identification process. With these assumptions, the new approximate model of the composite load is shown in Fig. 2.

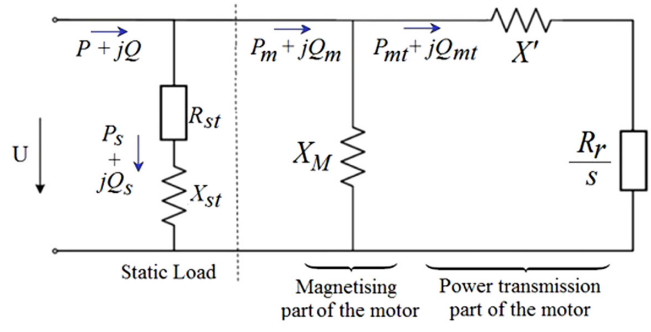

Fig. 2 . Simplified composite load with a modified motor model.

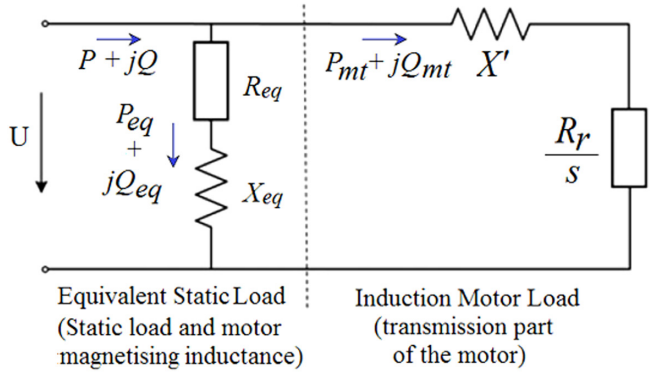

Fig. 3 . Simplified composite load circuit.

As a result, the induction motor part of the load model can be represented in two parts as "magnetizing part" and "power transmission part" as shown in Fig. 2. X_M is a negligible term in the motor part since the value of magnetizing reactance is much greater than the other reactances of the motor in practice and therefore, the current on it is much smaller. Besides, since X_M essentially exhibits an impedance behavior, it can be displayed in the static impedance part of the load. Thus, the static load and the magnetizing reactance are represented as an equivalent impedance as follows:

$$R_{eq} + jX_{eq} = jX_M // \left(R_{st} + jX_{st}\right) \quad (3)$$

Additionally considering that $X \gg X'$, $\omega_r \simeq 1$ and $A + B + C = 1$, the motor part of the model shown in Fig. 3 can be further simplified as

$$\begin{aligned}\frac{dE_d}{dt} &= -\frac{\omega_0 R_r}{X'}\left(E_d - U_d\right) + \omega_0 s E_q \\ \frac{dE_q}{dt} &= -\frac{\omega_0 R_r}{X'}\left(E_q - U_q\right) - \omega_0 s E_d \\ \frac{ds}{dt} &= -\frac{1}{H}\left(P_{mt} - P_{mt0}\right)\end{aligned} \quad (4)$$

Stator currents I_d and I_q are given as

$$I_d = \frac{U_q - E_q}{X'};\ I_q = \frac{E_d - U_d}{X'} \quad (5)$$

Active and reactive powers drawn by the motor (power transmission part) are given as follows:

$$P_{mt} = U_d I_d + U_q I_q;\quad Q_{mt} = -U_d I_q + U_q I_d \quad (6)$$

It must be noted here that the reactive power in (6) does not include the reactive power drawn by the magnetization impedance since it is included in the reactance X_{eq}. Furthermore, the following equations for the active, reactive and apparent power in the power transfer part of the motor, which are valid for steady-state conditions, will be used in load identification:

$$P_{mt0} = \frac{R_r}{s_o} I_0^2$$
$$Q_{mt0} = X' I_0^2 \quad (7)$$
$$P_{mt0}^2 + Q_{mt0}^2 = U_0^2 I_0^2$$

At this point, it will be informative to discuss the similarities and differences between the active and reactive powers (P_m, Q_m) drawn by the motor in Fig. 1 and the active and reactive powers (P_{mt}, Q_{mt}) of the power transmission part of the motor presented in Fig. 3: (1) Active powers are very close to each other ($P_m \approx P_{mt}$) and (2) Since the main reactive power of the motor is in the magnetizing reactance, the reactive power Q_m drawn by the motor is much bigger than the reactive power in the power transfer part of the motor ($Q_m \gg Q_{mt}$).

Based on these assumptions, it can be assumed that the current drawn by the power transmission part of the motor is proportional to the active power drawn by the motor. It must be stated here that the state variables of the model are *d*- and *q*-axis transient electromotive forces E_d and E_q, rotor slip *s*, and current of equivalent reactance X_{eq}. Model response to any further event can be obtained by set of equations in (4) and (8):

$$\frac{d}{dt} i_{eq\_d} = \frac{1}{L_{eq}} \left(U_d - R_{eq} i_{eq\_d} + L_{eq} \omega_0 i_{eq\_q} \right)$$
$$\frac{d}{dt} i_{eq\_q} = \frac{1}{L_{eq}} \left(U_q - R_{eq} i_{eq\_q} - L_{eq} \omega_0 i_{eq\_d} \right) \quad (8)$$

where i_{eq} is current on impedance $R_{eq}+jX_{eq}$ at rotor reference frame.

III. PARAMETER IDENTIFICATION OF THE LOAD MODEL

In this study, the model parameters are identified in two steps. In the first step, the steady-state values before and after voltage sag/swell events that occur at least one or more times are used, and with these data, the equivalent impedance in Fig. 3 and the transient reactance values of the motor are identified. In the second step, the rotor resistance of the motor and mechanical rotation inertia parameters is identified by using the instantaneous measurement data of only one event, and the rotor slip values are estimated. Since this method does not contain cyclic or loop operations based on trial and error, the amount of calculation is low and has a forward-oriented algorithm. The steps involved in determining the model parameters are given in Fig. 4.

A. Parameter Identification of Static Impedance and Transient Reactance of the Motor

In this first step, only pre- and post-event steady-state measurement values are used for voltage sag or swell events. The values that can be measured are the network voltages and the active and reactive powers of the load. However, symmetrical component analysis is processed, and positive sequence components of active and reactive values are used for identification. After estimating the impedance part of the load and the active and reactive powers drawn by the motor part from the measured values, the values of the impedance part of the load and the transient reactance of the motor can be identified. First of all, some assumptions are required in order to estimate the active and reactive powers drawn by the induction motor and impedance parts of the load. The assumptions developed step by step for steady-state conditions in this study are as follows:

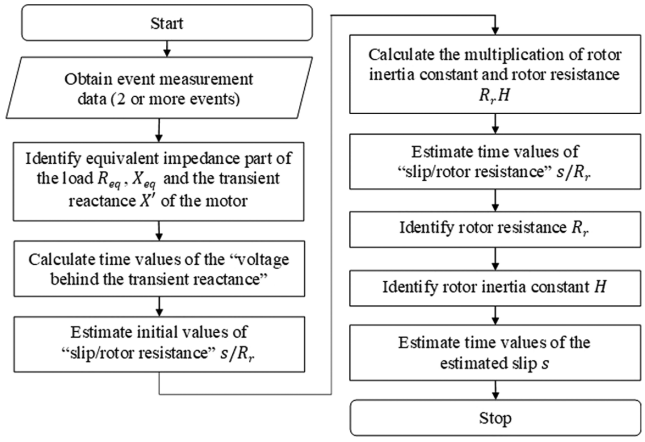

Fig. 4. Algorithm for identification of model parameters.

i) Positive sequence components of active and reactive power of the equivalent impedance part of the load are expected to be approximately proportional to the square of the busbar voltage at steady-state ($P_{eq0}^+ \propto U_0^2$, $Q_{eq0}^+ \propto U_0^2$).

ii) At the steady-state condition, it is observed that the effect of the busbar voltage level on the active power drawn by the motor is quite low. The active power values drawn by the motor part before and after the event are very close to each other. Such a feature is observed because the power demand of the mechanical load is not affected much by the voltage sag/swell and the motor continues to operate to meet the mechanical load demand. Although the active power values of the motor are very close to each other, also a difference can be explained by the thermal losses in the resistances and the effect of the mechanical load. Therefore, it is assumed that a significant part of the active power drawn by the motor part is a constant value ($P_{mt0}^+ \cong y_{p2}$, where y_{p2} is a constant value).

iii) Since the active power of the induction motor does not change much with respect to the voltage changes and there is a small amount of reactive power in the motor power transfer part, it can be assumed that the current drawn by the motor power transmission part in a given operating range is inversely proportional to the busbar voltage ($I_0 \propto U_0^{-1}$).

iv) The reactive power drawn by the motor power transmission part depends on the transient reactance X' ($Q_{mt0}^+ = X' I_0^2$) . Therefore, the reactive power of the motor power transmission part is inversely proportional to the square of the busbar voltage ($Q_{mt0}^+ \propto U_0^{-2}$ or $Q_{mt0}^+ \cong y_{q2} U_0^{-2}$ where y_{q2} is a constant value).

v) The amount of reactive power drawn by the impedance part of the load is expected to be proportional to the square of the grid voltage ($Q_{eq0}^+ \cong y_{q1} U_0^2$, where y_{q1} is a constant value).

Finally, the active and reactive powers drawn by the load are the sum of the powers drawn by the two parts of the load:

$$\begin{aligned} P_0^+ &= P_{eq0}^+ + P_{mt0}^+ \\ Q_0^+ &= Q_{eq0}^+ + Q_{mt0}^+ \end{aligned} \tag{9}$$

The subscript "0" in (9) denotes the steady-state values of the attributes. Based on these features and assumptions, any arrays $Y_p = [y_{p1}, y_{p2}]^T$ and $Y_q = [y_{q1}, y_{q2}]^T$ with constant elements, the following equations can be written:

$$\begin{aligned} P_{eq0}^+ &= y_{p1} U_0^2 \\ Q_{eq0}^+ &= y_{q1} U_0^2 \\ P_{mt0}^+ &= y_{p2} \\ Q_{mt0}^+ &= y_{q2} U_o^{-2} \end{aligned} \tag{10}$$

Substituting these expressions in (9), the following equations are obtained:

$$\begin{aligned} P_0^+ &= y_{p1} U_o^2 + y_{p2} \\ Q_0^+ &= y_{q1} U_o^2 + y_{q2} U_o^{-2} \end{aligned} \tag{11}$$

At least voltage sag/swell events must occur in order to solve these equations. If the values to be used in the solution for different steady-state voltage levels as a result of the events that occur are enumerated, the following equations in a compact form are obtained:

$$\underbrace{\begin{bmatrix} P_{01}^+ \\ P_{02}^+ \\ \vdots \\ P_{0N}^+ \end{bmatrix}}_{P} = \underbrace{\begin{bmatrix} U_{01}^2 & 1 \\ U_{02}^2 & 1 \\ \vdots & \vdots \\ U_{0N}^2 & 1 \end{bmatrix}}_{U_a} \underbrace{\begin{bmatrix} y_{p1} \\ y_{p2} \end{bmatrix}}_{Y_p}; \underbrace{\begin{bmatrix} Q_{01}^+ \\ Q_{02}^+ \\ \vdots \\ Q_{0N}^+ \end{bmatrix}}_{Q} = \underbrace{\begin{bmatrix} U_{01}^2 & U_{01}^{-2} \\ U_{02}^2 & U_{02}^{-2} \\ \vdots & \vdots \\ U_{0N}^2 & U_{0N}^{-2} \end{bmatrix}}_{U_a} \underbrace{\begin{bmatrix} y_{q1} \\ y_{q2} \end{bmatrix}}_{Q_p} \tag{12}$$

or

$$Y_P = \left(U_a^T U_a\right)^{-1} U_a^T P \tag{13}$$

$$Y_Q = \left(U_a^T U_a\right)^{-1} U_a^T Q$$

According to this formulation, at least two voltage level values are required and, in this case, steady-state data of at least an event is required. The voltage, active, and reactive powers are measured values, and from the values obtained from the solution of the equations, the equivalent impedance and transient reactance parameters are found:

$$y_{p1} = \frac{R_{eq}}{|Z_{eq}|^2}; y_{q1} = \frac{X_{eq}}{|Z_{eq}|^2}; y_{q2} = Q_{mt0}^+ U_0^2 = X' U_0^2 I_0^2 \tag{14.a}$$

or equivalently,

$$|Z_{eq}| = \sqrt{y_{p1}^2 + y_{q1}^2}; R_{eq} = y_{p1} |Z_{eq}|^2; X_{eq} = y_{q1} |Z_{eq}|^2 \tag{14.b}$$

equations are obtained. After R_{eq} and X_{eq} are identified, the equivalent impedance and then the stator current of the induction motor are calculated. After the steady-state current of the motor I_0 is found, the transient reactance is obtained as described below:

$$X' = \frac{y_{q2}}{U_0^2 I_0^2} \tag{15}$$

B. Parameter Identification of Motor Side

Once the parameter X' is obtained, the voltage values behind the transient reactance are obtained as a function of time:

$$\begin{aligned} E_d(t) &= U_d(t) + X' I_q(t) \\ E_q(t) &= U_q(t) - X' I_d(t) \end{aligned} \tag{16}$$

Let s_r be the ratio of slip to rotor resistance with slip s:

$$s_r(t) = \frac{s(t)}{R_r} \tag{17}$$

At the steady-state, the ratio of slip/rotor resistance s_{r0} is given below:

$$s_{r0} = \frac{s_0}{R_r} = \frac{I_{d0}}{E_{d0}} = \frac{I_{q0}}{E_{q0}} \tag{18}$$

is valid and from these equations above the initial values of $s_r(t)$ are determined before the event. It is possible to write the power equation as follows for any event where t_a is the start and t_b is the ending time of the event:

$$s_r(t) = s_r(t_b) - \frac{1}{R_r H} \int_{t_a}^{t_b} \left(P_{mt}^+(t) - P_{mt0}^+\right) \tag{19}$$

With this equation, instantaneous values of $s_r(t)$ during the event are estimated. After that, it becomes possible to identify the rotor resistance. State equations regarding voltages can be written as

$$\frac{dE_d}{dt} = R_r \left(-\frac{\omega_0}{X'} \left(E_d - U_d\right) + \omega_0 s_r E_q \right) \tag{20}$$

$$\frac{dE_q}{dt} = R_r \left(-\frac{\omega_0}{X'} \left(E_q - U_q\right) - \omega_0 s_r E_d \right)$$

Since the voltage values are obtained instantaneously, the identification process becomes easier. After labeling the integrals as

$$A_d = \int_{t_a}^{t_b} \left(-\frac{\omega_0}{X'} \left(E_d(t) - U_d(t)\right) + \omega_0 s_r(t) E_q(t) \right) dt \tag{21}$$

$$A_q = \int_{t_a}^{t_b} \left(-\frac{\omega_0}{X'} \left(E_q(t) - U_q(t)\right) - \omega_0 s_r(t) E_d(t) \right) dt$$

the rotor resistance can be identified as follows:

$$R_r = \sqrt{\frac{\left(E_d(t_a) - E_d(t_b)\right)^2 + \left(E_q(t_a) - E_q(t_b)\right)^2}{A_d^2 + A_q^2}} \quad (22)$$

After the rotor resistance is identified, slip values are obtained using (17).

It must be emphasized here that all equations have been developed for the identification of parameters of a composite load. The model of induction motor is a part of this composite load. The composite load model consists of an RL impedance and an induction motor. Impedance is a serially connected resistance and an inductance, which means an impedance of $\left(R_{st} + jX_{st}\right)$. The motor magnetizing impedance jX_m and RL impedance, which are considered to be connected parallel to each other, constitutes an equivalent impedance of $R_{eq} + jX_{eq}$. Moreover, the important parameters of the motor and the equivalent impedance part were identified. The identified motor parameters are X' (transient reactance of the motor), R_r (rotor resistance of the motor), and H or J (Rotor inertia constant) While the identified impedance parameter are R_{eq} and X_{eq}. In summary, the model has four state variables and five parameters. These 5 parameters are identified in the identification process through Eqs. (9)–(22). After identification is executed and parameters are obtained, model response to any event is obtained by Eqs. (4) and (8).

IV. RESULTS

Three case studies have been investigated to illustrate the performance of the method. The first study deals with a load consisting of only one impedance and an induction motor. The purpose of this case study is to show how accurately the method can estimate parameters and to investigate how to estimate the load behavior. In the second case study, the estimation performance of the method to a more realistic load is examined. In this study, the load consists of a voltage-reducing transformer, multiple impedances and induction motors, and reactive power compensators as well. The third case study shows the method's contribution in determining the cause of an event. In this study, a network consisting of a voltage supply and two loads is considered. The loads consist of a voltage-reducing transformer, multiple impedances and induction motors, and reactive power compensators as in case study 2. Both in studies 2 and 3, the measurements are taken on the high voltage side of the transformer connected to the network, since data are more available on the network side.

A. Case Study 1 Composite Load Consisting of an Impedance and an Induction Motor

The parameters of the impedance and the induction motor are given as: the impedance: $R_{st} = 19.2\ \Omega$ and $X_{st} = 10.8573\ \Omega$. The induction motor data: 3 *HP*, 220 V_{LL}, 60 Hz, $X_{ls} = X_{lr} = 0.7540\ \Omega$, $X_m = 26.012\ \Omega$, $R_s = 0.435\ \Omega$, $R_r = 0.816\ \Omega$, $J = 0.089\ \text{kg·m}^2$. The load with these parameters will have equivalent impedance and transient reactance values as follows: $Z_{eq} = 7.5182 + j11.5752\ \Omega = 13.802\ \angle\ 56.996^0\ \Omega$, $X' = 1.486\ \Omega$, the rated rotational inertia of the motor is $T_L = 11.9$ N.m.

Event 1: While the amount of load $T_L = 11.9$ N m is applied to the rotor, a voltage drop event occurs at $t = 1.0$ s with a different depth of 9.1%, 22.73%, and 4.55% (20 V, 50 V, and 10 V drop) for each phase. With the data of this event, the parameters of the load model were estimated using the proposed method and the following values were obtained: $Z_{eq} = 7.928273 + j11.663606\ \Omega = 14.103\ \angle\ 55.794^\circ\ \Omega$, $X' = 1.2744\ \Omega$, $R_r = 0.9407\ \Omega$, $J = 0.08609$ kg m^2. It is clear that estimated parameters are very close to the real values. Moreover, in Fig. 5, the active and reactive powers drawn by the load and the results of the estimation of the model are shown for the case of voltage drop at $t = 1.0$ s to illustrate the accuracy of the method. It is clear from Fig. 5 that the real and reactive power estimated (solid red line) closely follows the actual ones (solid blue line). At steady-state, the error rate in active and reactive power estimation of the total load is 0.0104% and 0.01737%, respectively. Although its parameters are obtained with a certain error rate, the estimation results on the active and reactive powers of the model are more satisfactory. The identification process was executed within 0.17782 s using data sampled 2000 samples/second by a personal computer having Intel(R) Core(TM) i5-10210U CPU @ 1.60GHz microprocessor and 16 GB RAM.

Event 2: The model can identify the load when a much deeper voltage sag has occurred. In case of voltage drop at phases are 45%, 18% and 36% (100 V, 40 V and 80 V drop), following values were obtained: $Z_{eq} = 8.046430 + j11.406010\ \Omega = 13.802\ \angle\ 56.996^\circ\ \Omega$, $X' = 1.411\ \Omega$, $R_r = 0.973\ \Omega$, $J = 0.0752\ \text{kg.m}^2$. At steady-state, the error rate in active and reactive power estimation of the total load is 0.91% and 1.75%,

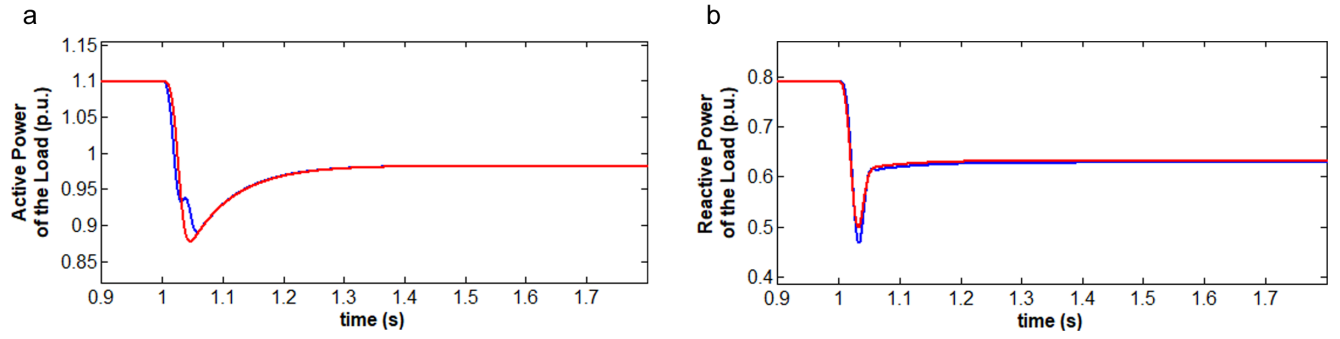

Fig. 5. Comparison of the actual and estimated real and reactive powers for case study 1, event 1: (a) actual and estimated active power and (b) actual and estimated reactive power (actual and estimated powers are presented in blue and red, respectively).

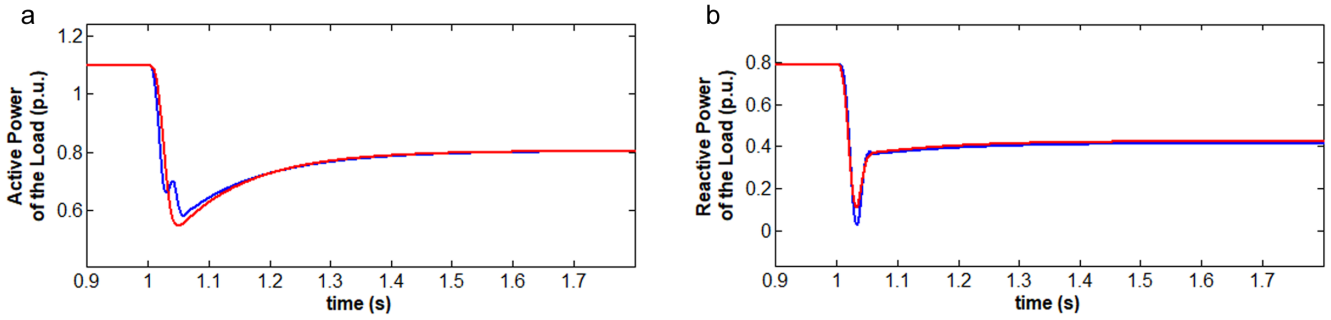

Fig. 6. Comparison of the actual and estimated real and reactive powers for case study 1, event 2: (a) actual and estimated active power and (b) actual and estimated reactive power (actual and estimated powers are presented in blue and red, respectively).

respectively, which shows that the less deep voltage sag results in better estimation. Results are presented in Fig. 6.

While discussing the performance of the proposed method, it is also necessary to estimate the parameter for different values of the network voltages, motor mechanical loads, and for several voltage sag/swell depths. In order to fulfill this requirement, firstly the network voltages and then the load of the motor and the depth of voltage drop are changed individually, and the results were compared. The estimated parameters of motor and impedance part obtained for different network voltage between 190 V and 260 V at a step of 10 V are shown in Table I. Z_{eq} =13.802∠56.996°Ω is the real and $Z_{eq(est)}$ is the estimated value of the equivalent impedance. Parameters are identified with a percentage error of 1.5% for the equivalent impedance $Z_{eq(est)}$, 11% for the rotor resistance $R_{r(est)}$, 4.4%, for mechanical inertia $J_{(est)}$, and *2–7%* for the transient reactance $X'_{(est)}$.

B. Case Study 2 Multiple Impedances and Induction Motors

Case 1 focuses on the identification of load parameters for a single impedance and induction motor. In practice, loads consist of many components and are compensated by compensation units. In this case study, the load to be identified is consists of 11 different impedances and 7 different induction motors having different parameters and mechanical loads and the load is compensated with a 0.85 power factor compensation. Additionally, it is considered that the composite load is connected to the grid by a transformer, and the measurement values are taken from the grid side of the transformer. The load is fed by 460 V (*L-L*), and its operating power is 390 kW. In Fig. 7, active and reactive powers drawn by the load and the estimation results of the model are shown for a voltage sag with different depths of 30%, 15%, and 5% (138 V, 69 V, and 23 V drop) for each phase at $t = 1.0$ s. At the steady-state condition, the error rate in active and reactive power estimation are found to be 0.1745 % and 1.857 %, respectively. As clearly seen in Fig. 7, the real and reactive powers estimated using the proposed method (solid red line) closely follow the actual real and reactive powers (solid blue line). In this case study, the load to be identified consists of more than one motor and impedance with different parameters as in real situations. Since the direct calculation of the motor-impedance load parameters equivalent to the identified load is another research subject in itself, the comparison of the estimated parameters has not been made here. Instead, the comparison for this case is performed only in terms of the real and reactive power estimation.

TABLE I.
ESTIMATED PARAMETERS FOR DIFFERENT GRID VOLTAGE LEVELS

Voltage *L-L* (V)	$X'_{(est)}$ (Ω)	$R_{r(est)}$ (Ω)	$J_{(est)}$ (kg m²)	$Z_{eq(est)}$ (Ω)
190	1.395	0.939	0.081	13.902∠55.267°
200	1.342	0.919	0.084	14.042∠56.060°
210	1.363	0.915	0.084	14.029∠56.133°
220	1.391	0.912	0.084	13.999∠56.083°
230	1.414	0.906	0.084	13.978∠56.047°
240	1.429	0.900	0.085	13.965∠56.028°
250	1.439	0.894	0.085	13.958∠56.022°
260	1.446	0.888	0.085	13.953∠56.022°

C. Case Study 3 Identification of the Cause of an Event

This case study is considered to show the contribution of the method in determining the cause of an event. The main idea is to use load models to detect whether the load is changed. If a load and its model's responses match, then it can be deduced that this load is not changed. However, if the load's response and its model's response do not match from the beginning of a moment, it can be deduced that the load is changed at this moment and probably causes an event. A simple network shown in Fig. 8 is considered to have two loads are connected to a supply through lines. Loads have the same ratings as in case 2.

The aim of this study is to detect the cause of an event occurring at a time interval of 1.0–1.05 s. At this time interval, two large induction motors are started by closing their circuit breaker at load 2, and at time 1.05 s, circuit breakers are opened. These turning on and turning off of induction motors cause events in the network which affect load 1. After events occurred, if measurement data is not recorded, it is not possible to find which load has temporarily changes and causes an event since both loads seem to be unchanged after the event has occurred. From the models' responses, we can detect which one has changed and caused the event.

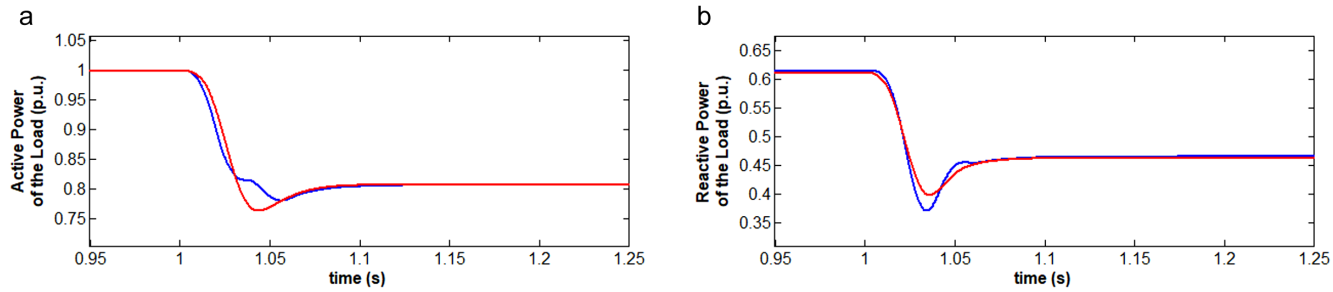

Fig. 7. Comparison of the actual and estimated real and reactive powers for case study 2: (a) actual and estimated active power and (b) actual and estimated reactive power (actual and estimated powers are presented in blue and red, respectively).

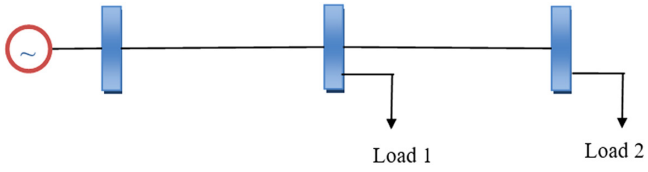

Fig. 8. The network is considered in case study 3.

The scenario considered is as follows: Between 0.3 s and 0.7 s a voltage sag event occurs. At 1.0 s, one of the large motor's circuit breakers of load 2 is closed, and at 1.05 s the circuit breakers are opened and load 2 remains as it was in before the time 1.0 s. After 1.05 s, Load 2 has the same characteristics as before and now it is not possible to find out if the load is changed and caused an event by steady-state measurement values after the event occurred. Referring to load models, it can be deduced when and if the load is changed.

In Fig. 9, actual and model responses of loads 1 and 2 are shown. Fig. 9a and 9b show the actual and estimated active and reactive power of load 1, and Fig. 9c and 9d show the actual and estimated active and reactive power of load 2 (actual and estimated values are represented by blue and red colors, respectively). Active and reactive power estimations of load 1 are quite close to actual values during the event as clearly seen in Fig. 9a and 9b. However, since the model of load 2 is changed temporarily between time 1.0 s and 1.05 s, active and reactive power estimation of its response by its model is wrong at this time interval. Actual load and model responses do

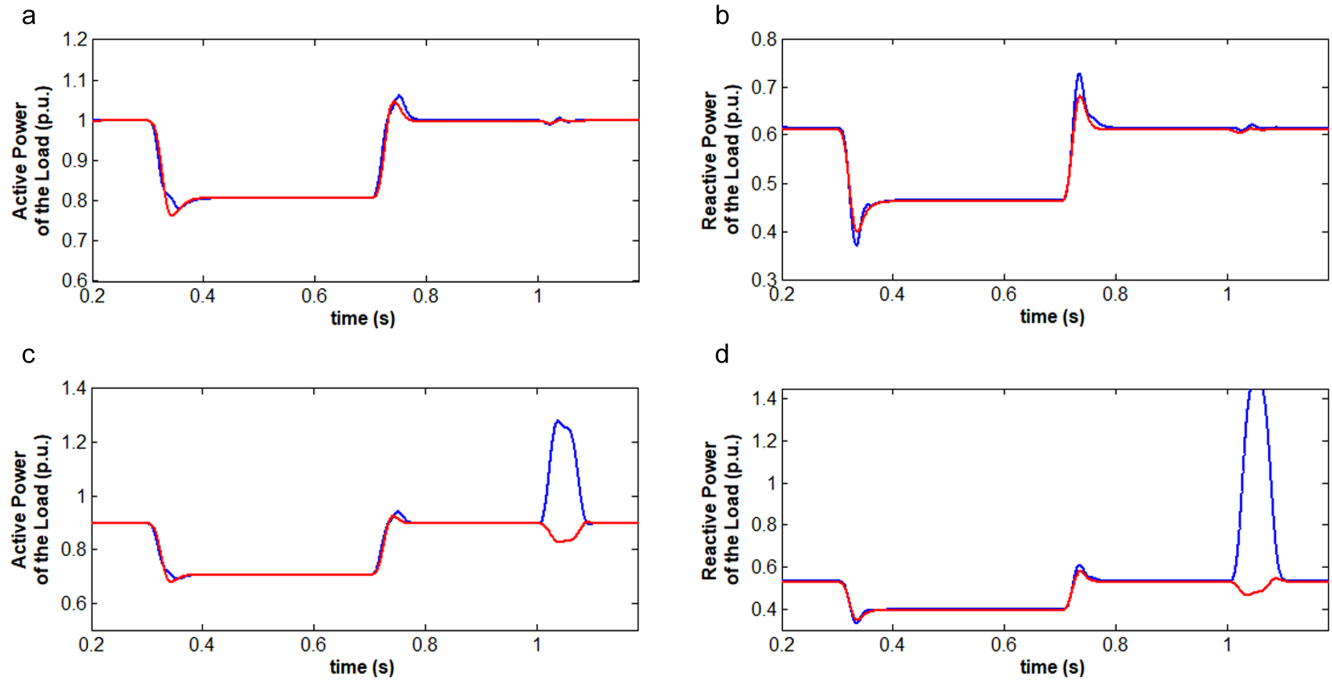

Fig. 9. Comparison of the actual and estimated real and reactive powers during event 1 at the time between 0.3 s and 0.7 s, and event 2 at the time between 1.0 s and 1.05 s of case study 3: (a) actual and estimated active power of load 1, (b) actual and estimated reactive power of load 1, (c) actual and estimated active power of load 2, and (d) actual and estimated reactive power of load 2 (actual and estimated powers are presented in blue and red, respectively).

TABLE II.
ESTIMATED PARAMETERS FOR DIFFERENT MOTOR MECHANICAL LOADS

Torque (Nm)	$X'_{(est)}$ (Ω)	$R_{r(est)}$ (Ω)	$J_{(est)}$ (kg m²)	$Z_{eq(est)}$ (Ω)
7.9	1.429	0.893	0.084	13.963∠56.079°
9.9	1.411	0.904	0.084	13.978∠56.083°
11.9	1.391	0.912	0.084	13.999∠56.083°
13.9	1.371	0.915	0.085	14.026∠56.081°
15.9	1.350	0.915	0.084	14.060∠56.078°

TABLE III.
ESTIMATED PARAMETERS FOR DIFFERENT VOLTAGE SAG DEPTHS

Sag Depth (V)	$X'_{(est)}$ (Ω)	$R_{r(est)}$ (Ω)	$J_{(est)}$ (kg m²)	$Z_{eq(est)}$ (Ω)
10	1.426	0.909	0.087	13.963∠55.953°
20	1.400	0.913	0.084	13.992∠56.060°
30	1.377	0.916	0.082	14.016∠56.130°
40	1.346	0.917	0.079	14.048∠56.220°
50	1.304	0.914	0.077	14.094∠56.344°

not match, and it can be deduced that structure of the load 2 has changed at this interval and this causes an event.

V. CONCLUSION

In this study, a load model has been proposed to estimate the response of network loads in response to network events and a method has been developed to estimate the parameters of this model. The aim of this model is to estimate the behavior of a load under power quality events. The feature of the method is to identify the parameters of the composite load model with less processing time by using measurement data from a voltage sag/swell. At least one sequential voltage sag/swell event is required to determine the parameters. In the case studies, it has been observed that the composite load model consisting of impedance and an induction motor gives results close to the actual load response. It is observed that the best results obtained by the developed method are obtained when the voltage sag/swell depth is less than 20%. Once the load model is obtained, it can be estimated how the load will behave under the occurrence of event such as voltage sag, voltage swell, or interruptions.

TABLE IV.
ESTIMATED PARAMETERS FOR DIFFERENT VOLTAGE SWELL DEPTHS

Swell Depth (V)	$X'_{(est)}$ (Ω)	$R_{r(est)}$ (Ω)	$J_{(est)}$ (kg m²)	$Z_{eq(est)}$ (Ω)
10	1.473	0.930	0.094	13.963∠55.951°
20	1.475	0.924	0.098	13.992∠56.057°
30	1.478	0.919	0.103	14.016∠56.127°
40	1.482	0.914	0.108	14.048∠56.218°

Peer-review: Externally peer-reviewed.

Declaration of Interests: The authors have no conflicts of interest to declare.

Funding: The authors declared that this study has received no financial support.

REFERENCES

1. U. Arumugam, N. M. Nor, and M. F. Abdullah, "A brief review on advances of harmonic state estimation techniques in power systems," *Int. J. Inf. Electron. Eng.*, vol. 1, no. 3, pp. 217–222, 2011. [CrossRef]
2. IEEE Task Force on Load Representation Performance, "Load representation for dynamic performance analysis (of power systems)," *IEEE Trans. Power Syst.*, vol. 8, no. 2, pp. 472–482, 1993. [CrossRef]
3. H. Renmu, M. Jin, and D. J. Hill, "Composite load modeling via measurement approach," *IEEE Trans. Power Syst.*, vol. 21, no. 2, pp. 663–672, 2006. [CrossRef]
4. S. Peerez-Londono, L. Rodriguez-Garcia, and J. Mora-Flores, "A comparative analysis of dynamic load models for voltage stability studies," In *Proceedings of 2014 IEEE PES Transmission & Distribution Conference and Exposition, Latin America (PES T&D-LA 2014)*, Medellin, Colombia, September 10—13, 2014, pp. 1–6.
5. X. Qu, X. Li, J. Song, and C. He, "An extended composite load model taking account of distribution network," *IEEE Trans. Power Syst.*, vol. 33, no. 6, pp. 7317–7320, 2018.
6. L. Li, X. Xie, J. Yan, and Y. Han, "Fast online identification of the dominant parameters of composite load model using Volterra model and pattern classification," In *Proceedings of 2007 IEEE Power Engineering Society General Meeting*, Tampa, FL, USA, June 24-–28, 2007, pp. 1–8.
7. S. Yu, S. Zhang, and X. Zhang, "Two-step method for the online parameter identification of a new simplified composite load model," *IET Gener. Transm. Distrib.*, vol. 10, no. 16, pp. 4048–4056, 2016. [CrossRef]
8. M. Rasouli, R. Sabzehgar, and H. R. Teymour, "An efficient approach for measurement-based composite load modeling," In *Proceedings of 2018 IEEE Energy Conversion Congress and Exposition (ECCE)*, Oregon, Portland, September 23-–27, 2018, pp. 7310–7314.
9. L. Rodriguez-Garcia, S. Perez-Londone, and J. J. Mora-Florez, "Methodology for measurement-based load modeling considering integration of dynamic load models," In *Proceedings of 2020 IEEE International Autumn Meeting on Power, Electronics and Computing*, Ixtapa, GRO, México: ROPEC, November 4-–7, 2020, pp. 1–6.
10. H. Marma, and X. Liang, "Composite load model and transfer function based load model for high motor composition load," In *Proceedings of 2019 IEEE Canada Electrical Power and Energy Conference (EPEC)*, Montreal, Canada, 2019, pp. 1–5.
11. F. Bu, Z. Ma, Y. Yuan, and Z. Wang, "WECC composite load model parameter identification using evolutionary deep reinforcement learning," *IEEE Trans. Smart Grid*, vol. 11, no. 6, pp. 5407–5417, 2020. [CrossRef]
12. Z. Ma, Z. Wang, Y. Wang, R. Diao, and D. Shi, "Mathematical representation of WECC composite load model," *J. Mod. Power Syst. Clean Energy*, vol. 8, no. 5, pp. 1015–1023, 2020. [CrossRef]

13. R. Venkatraman, S. K. Khaitan, and V. Ajjarapu, "Application of combined transmission-distribution system modeling to WECC composite load model," In *Proceedings of 2018 IEEE Power & Energy Society General Meeting (PESGM)*, Portland, Oregon, August 5–9, 2018, pp. 1–5.
14. Z. Ma, B. Cui, Z. Wang, D. Zhao, and D. Zhao, "Parameter reduction of composite load model using active subspace method," *IEEE Trans. Power Syst.*, vol. 36, no. 6, pp. 5441–5452, 2021. [CrossRef]
15. I. A. Hiskens, "Nonlinear dynamic model evaluation from disturbance measurements," *IEEE Trans. Power Syst.*, vol. 16, no. 4, pp. 702–710, 2001. [CrossRef]
16. Q. Liu, Y. Chen, and D. Duan, "The load modeling and parameter identification for voltage stability analysis," In *Proceedings of 2002 International Conference on Power System Technology*, Kunming, China, October 13–17, 2002, pp. 2030–2033.
17. X. Zhang, C. Lu, and Y. Wang, "Identifiability analysis of load model parameter identification with likelihood profile method," In *Proceedings of 2018 IEEE Power & Energy Society General Meeting (PESGM)*, Portland, Oregon, August 5–9, 2018, pp. 1–5.
18. M. E. Jahromi, and M. T. Ameli, "Measurement-based modelling of composite load using genetic algorithm," *Electr. Power Syst. Res.*, vol. 158, pp. 82–91, 2018. [CrossRef]
19. X. Li, L.Wang, and P. Li, "The study on composite load model structure of artificial neural network," In *Proceedings of Third International Conference on Electric Utility Deregulation and Restructuring and Power Technologies*, Nanjing, China, April 6–9, 2008, pp. 1564–1570.
20. V. Knyazkin, C. A. Canizares, and L. H. Soder, "On the parameter estimation and modeling of aggregate power system loads," *IEEE Trans. Power Syst.*, vol. 19, no. 2, pp. 1023–1031, 2004. [CrossRef]
21. C. Wang, Z. Wang, J. Wang, and D. Zhao, "Robust time-varying parameter identification for composite load modeling," *IEEE Trans. Smart Grid*, vol. 10, no. 1, pp. 967–979, 2019. [CrossRef]
22. K. O. Abledu, *Equivalent Load Model of Induction Machines Connected to a Common Bus*, Ph.D. dissertation. Iowa, US: Iowa State University, 1983.
23. S. Yu, S. Zhang, Y. Han, C. Lu, Z. Yu., and X. Zhang, "Fast parameter identification and modeling of electric load based on simplified composite load model," In *Proceedings of 2015 IEEE Power & Energy Society General Meeting*, Denver, Colorado, July 26–30, 2015, pp. 1–5.
24. P. Kundur, *Power System Stability and Control*. California: McGraw-Hill, 1993.
25. P. S. E. C. System Dynamic Performance Subcommittee. "Standard load models for power flow and dynamic performance simulation", *IEEE Trans. Power Syst.*, Vol. 10, no. 3, pp. 1302–1313, 1995.

Appendix

All symbols and variables in the text are defined as a list of nomenclature in the following:

Symbol	Explanation
f_0, ω_0	Base frequency and angular frequency of the power system
R_{st}, X_{st}	Resistance and reactance of the static impedance
R_{eq}, X_{eq}	Resistance and reactance of the equivalent static impedance
R_s, R_r	Stator and rotor resistance of the motor
X_S, X_R	Stator leakage and rotor leakage reactance of the motor
X_M	Magnetizing reactance of the motor
X	Stator circuit reactance
X'	Transient reactance of the motor
$T_0^{'}$	Transient open-circuit time constant
A,B,C	Constant torque coefficient
H	Rotor inertia constant
J	Rotor inertia coefficient
s	Slip of the motor
ω_r	Normalized rotor electrical speed
U,U_d,U_q	Bus voltage, d-axis, and q-axis bus voltage
I,I_d,I_q	Stator current, d-axis, and q-axis stator current
E,E_d,E_q	transient electromotive force, d-axis, and q-axis transient electromotive force
P,Q	Active and reactive power of the composite load
P_{st},Q_{st}	Active and reactive power of the static impedance
P_{eq},Q_{eq}	Active and reactive power of the equivalent static impedance
P_m,Q_m	Active and reactive power of the motor
P_{mt},Q_{mt}	Active and reactive power of the transmission part of the motor (excluding its magnetizing part)